Chemistry SELECT

www.chemistryselect.org

A journal of ChemPubSoc Europe

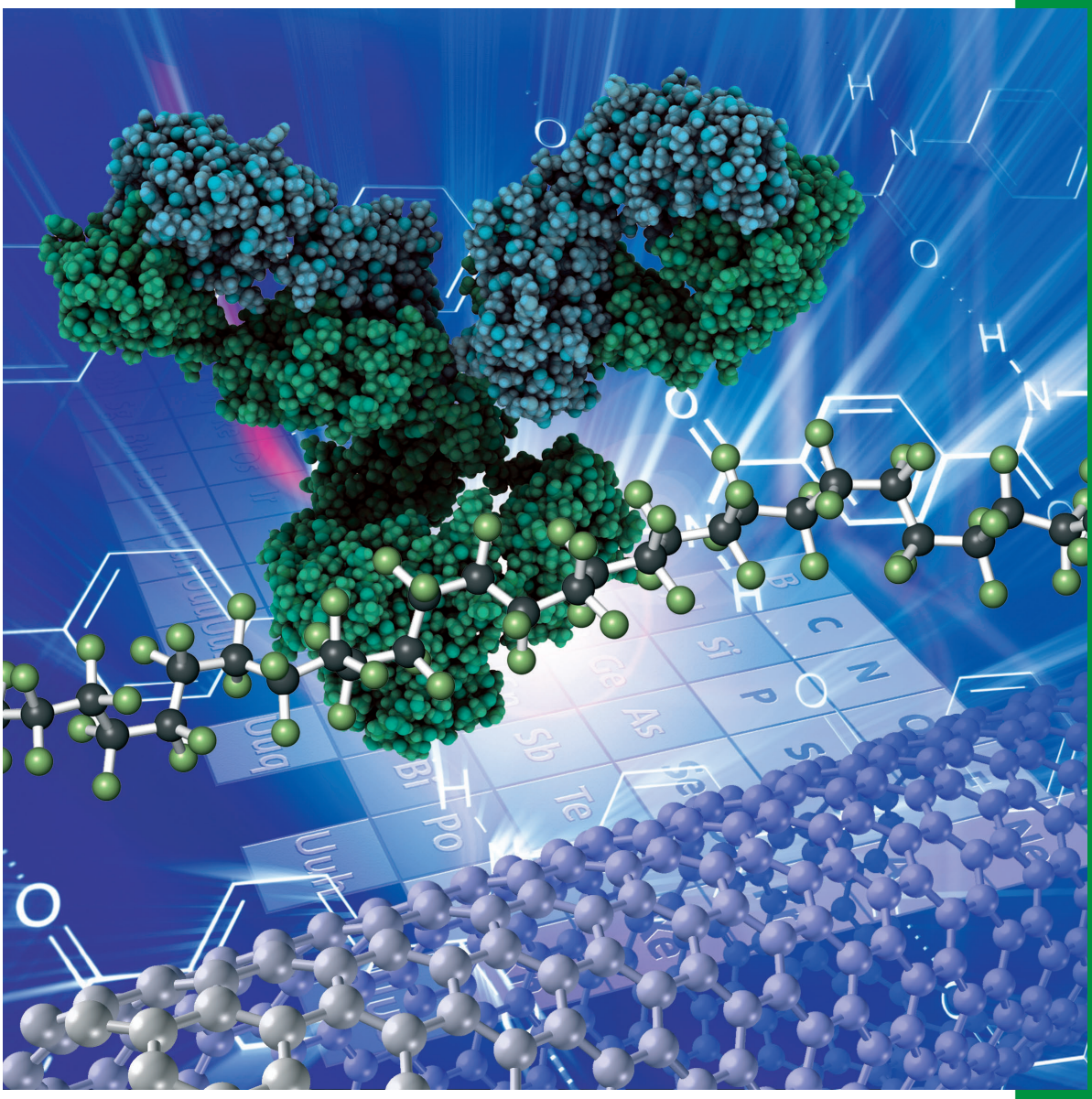

REPRINT

WILEY-VCH

ChemPubSoc Europe

DOI: 10.1002/slct.201802538

Chemistry SELECT Full Papers

Catalysis

Keto-Enol Tautomerism in Nucleobase-Substituted Aldols

Mariano J. Nigro,[a] Adolfo M. Iribarren,[a] Sergio L. Laurella,*[b] and Elizabeth S. Lewkowicz*[a]

Acyclic nucleosides, which exhibit significant antiviral activity, are usually synthesised using traditional chemical strategies. However, the efficient and selective formation of carbon-carbon bonds using small organic molecules as catalysts provides a promising alternative route for the sustainable synthesis of this family of compounds. Following this organocatalytic strategy, 5-(adenyl, thyminyl and cytosyl)-4-hydroxy-2-pentanones were prepared by the pyrrolidine catalysed reaction between the 2-oxoethyl derivative of the corresponding nucleobases and acetone. In order to investigate the keto-enol equilibrium of these compounds in basic media, *H-D* exchange studies were carried out by ^{1}H and ^{13}C NMR spectroscopy. The obtained results suggest that the mechanism by which this exchange occurs is of first order with respect to all the substrates, but of second order with regard to pyrrolidine in the case of the cytosine and adenine derivatives and of first order for the thymine analogue. Theoretical calculations of the structures involved in this equilibrium also suggest that the stability of the different ionic intermediates depends on the pK_a of the corresponding nucleobases.

Introduction

During the last decades, many nucleotide analogues have been synthesised and their biological activities tested.[1] The main therapeutic application of this family of compounds is in the field of antiviral agents, counting at the present with more than 30 drugs approved for numerous targets such as hepatitis, HIV and herpes virus infections.[2,3] Among these analogues, acyclic nucleosides (ANs) exhibit enhanced chemical and metabolic stability, acting mainly as chain terminators during DNA or RNA biosynthesis. The first known member of this family, acyclovir, displays extremely low toxicity for normal cells and a strong inhibitory activity against herpes simplex virus (HSV) being today the main drug for the treatment of this infection.[4] The subsequent development of a series of ANs with diverse side chains resulted in analogues such as ganciclovir, penciclovir, famciclovir, and adefovir[5] that showed improved solubility and oral bioavailability.

There is a permanent interest in the search of novel ANs with diminished host toxicity and broader therapeutic spectrum. The traditional strategy for the synthesis of ANs involves the complex and stereoselective preparation of the acyclic chain followed by the regioselective coupling to the nucleobase[6] affording poor yields and undesired waste. Taking into account these considerations, we have developed, for the synthesis of AN analogues, innovative catalytic routes based on organocatalysis[7] and biocatalysis.[8] In particular, organocatalysis has emerged as a promising area for the sustainable, efficient and selective carbon–carbon bond formation using small organic molecules as catalysts.[9–11] In contrast to biocatalysts, that are highly substrate specific, organocatalysts catalyse reactions with a wide range of substrates.[12] Additionally, these strategies allowed the successful achievement of a large number of asymmetric transformations. Among them, amine-catalysed chemo- and regioselective aldol additions have been applied to the synthesis of structurally interesting and biologically important natural products.[13,14] In the aldol reaction two carbonyl compounds, mainly one aldehyde with one ketone, react to create a new β-hydroxycarbonyl compound where the stereochemistry of the new chiral centre depends on the chirality of the employed organocatalyst. Regarding the organocatalyst, commercially available natural secondary amines were the most frequently explored.[15] For example, a novel approach for the enantioselective synthesis of the hydroxylated amino acid (2 *S*,3 *S*)-3-hydroxy-L-arginine, an intermediate in the biosynthesis of a tuberactinomycin peptide antibiotics constituent, included as key-step an aldol addition catalysed by L-proline.[16] The proposed mechanism involves the reaction of the pyrrolidine ring with the carbonyl group to generate an enamine intermediate. At present, new and more complex chiral catalysts with novel scaffolds are being developed.[17,18] Crivoi et al.[19] prepared nanohybrid materials based on L-leucine and hydrotalcites that were tested as organocatalysts in the aldol addition of cyclohexanone with different aromatic aldehydes. They observed that, although the reaction was complete after 1 h, there was a continuous interchange between the obtained *syn* and *anti* diastereoisomers that depended not only on the nature of the catalyst but also on the solvent used. They explained the observed behaviour by the strong basic sites present in the hydrotalcites which could promote the subtraction of an *H* atom in the α-position of the ketone favouring the equilibrium with the enol form in aqueous media.

[a] *M. J. Nigro, Dr. A. M. Iribarren, Dr. E. S. Lewkowicz*
Laboratorio de Biocatálisis y Biotransformaciones, Universidad Nacional de Quilmes, Roque Sáenz Peña 352, (1876) Bernal, Buenos Aires, Argentina
E-mail: elewko@unq.edu.ar

[b] *Dr. S. L. Laurella*
Laboratorio LADECOR, División Química Orgánica, Departamento de Química, Facultad de Ciencias Exactas, Universidad Nacional de La Plata, 47 y 115 (1900), La Plata, Buenos Aires, Argentina
E-mail: sllaurella@quimica.unlp.edu.ar

Supporting information for this article is available on the WWW under https://doi.org/10.1002/slct.201802538

In effect, keto-enol tautomerism has been observed in a wide variety of compounds such as aldehydes, ketones, β-dicarbonylic compounds, β-ketoesters, β-ketoamides, β-ketonitriles and numerous heterocycles.[20] There has been a considerable interest in the enolisation of carbonyl compounds for many years[21] and excellent methods have been developed for the generation of simple enols of aldehydes and ketones in solution.[22] Enolisation of carbonyl compounds is the rate-determining step in numerous organic reactions, such as electrophilic substitution to carbonyl compounds, Carrol rearrangement and retro-Diels Alder.[23] The enol isomers of simple monofunctional aldehydes and ketones are generally quite unstable and revert to their carbonyl tautomers rapidly. However, enols can be stabilised by different internal and external factors: interaction with solvent,[24] steric effects,[25] electronic stabilisation,[26] internal hydrogen bonds,[27] etc.

We have previously reported the synthesis of AN analogues using for the first time 2-oxoethyl derivatives of thymine and adenine (**1 a,b**, Scheme 1) as substrates for the organocatalysed

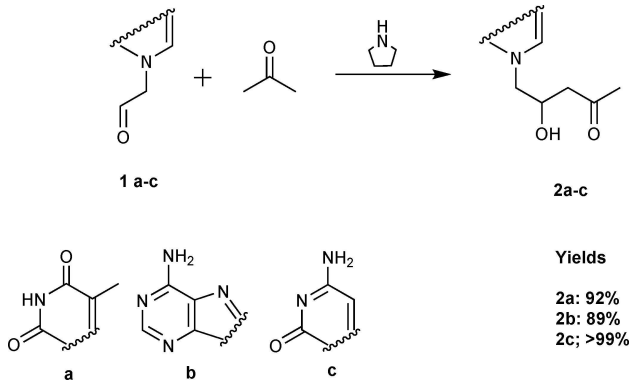

Scheme 1. Organocatalysed synthesis of *N*- 2-hydroxy-4-oxopentyl derivatives of nucleobases.

aldol addition reaction with acetone.[7] In this work we studied the intra- and intermolecular interactions that could influence the keto-enol equilibrium in the aldol moiety of the synthesised AN analogues, analysing the differences observed between purine and pyrimidine derivatives. We also optimised the yield of the synthesised aldols, extending the range of products by preparing the new cytosine derivative **2 c**.

Results and Discussion

Substrate synthesis

The aldehydic substrates used for the amine-organocatalysed aldol additions were prepared by regioselective *N*-alkylation of the corresponding nucleobases with 2-bromo-1,1-dimethoxyethane as previously reported.[7] Three structurally diverse nucleobases: thymine, adenine and cytosine were chosen as starting materials for the synthesis of the corresponding *N*-2-oxoethyl derivatives **1 a-c**, which were obtained in 40–60% yields. *N*1-alkylated products were mainly achieved in reactions with pyrimidine bases while adenine afforded the *N*9-alkylated derivative. Due to the intrinsic reactivity of the aldehyde group, the corresponding dimethyl acetals were first prepared and then deprotected just prior to their use. In aqueous solutions, these compounds exist mainly in two different forms, aldehyde and hydrate. Spectroscopic data showed that the equilibrium between these species depends on the pH of the medium and also on the involved nucleobase, which was explained considering different protonation sites.[28]

Organocatalysed reaction

The mild reaction conditions provided by organocatalytic approaches, allow the use of highly-reactive aldehydic substrates that would represent a drawback for other types of syntheses. Pyrrolidine-catalysed *C–C* bond formation between **1 a-c** and acetone was carried out at room temperature (Scheme 1), affording the aldol products **2 a-c** in conversions up to 99%, determined by HPLC (Figure S1) as racemic mixtures. After purification, aldol structures were confirmed by ^{13}C and ^{1}H NMR (Figures S2-S4). The three compounds showed similar signal profiles of the acyclic chain which were also in accordance with those observed in related compounds prepared using aldolases as biocatalysts.[8] In particular, the singlet at around 2.2 ppm (COC**H**$_3$) and the double double doublet at δ 2.6-2.8 ppm (C**H**$_2$CO, diastereotopics) in ^{1}H NMR spectra and the ^{13}C NMR signals at δ 30 ppm (CO**C**H$_3$) and 48 ppm (-**C**H$_2$CO), were keys for analysing the keto-enol equilibrium.

Fast H-D exchange equilibrium

The different physical and chemical properties as well as different three-dimensional shapes of tautomers, often leads to a selective binding to proteins.[29] With the aim of studying the keto-enol equilibrium of compounds **2 a-c**, their ^{1}H and ^{13}C NMR spectra in D_2O and pyrrolidine at different times were recorded. Although ^{1}H NMR spectra did not show signals that could be assigned to any of the possible tautomers of these compounds (**3** and **4**, Scheme 2), the integration of the signals correspond-

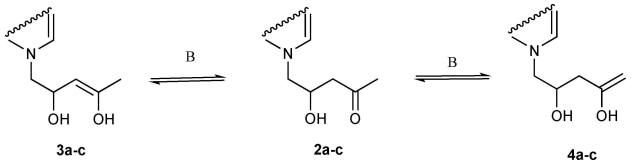

Scheme 2. Tautomers of compounds **2 a-c.**

ing to the α-hydrogens adjacent to the carbonyl group showed a progressive decrease. This behaviour would indicate that a fast *H-D* exchange is occurring as a result of the expected keto-enol equilibrium. Figure 1 shows the ^{1}H NMR spectra in the range 2–2.8 ppm and the ^{13}C NMR between 30 and 50 ppm for

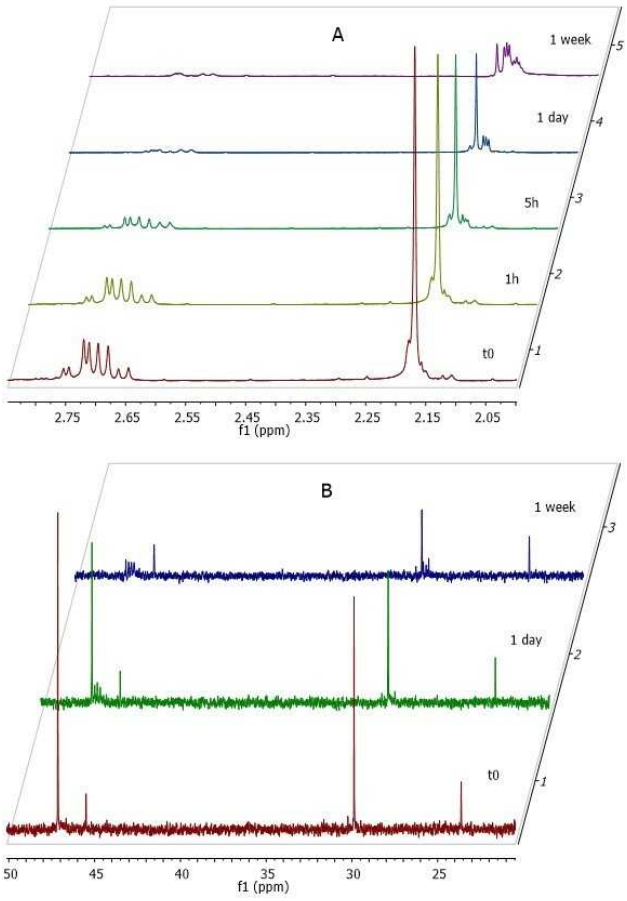

Figure 1. (A) ^{1}H and (B) ^{13}C NMR spectra of **2c** monitored for one week in D_2O. The detailed assignment of the signals is shown in Figure S4 and described in Experimental Section in the Supporting Information.

compound **1c** at different times. The reversible and fast formation of both compounds, **3** and **4**, leads to the incorporation of deuterium atoms at both sides of the carbonyl group after 1 week at differential rates. The occurrence of new signals and the change of multiplicities in ^{1}H and ^{13}C NMR spectra also confirmed the expected incorporation of deuterium.

The evolution of ($COCH_3$) and (CH_2CO) signal integration over time for compounds **2a-c** is shown in Figure 2 and Table S1. The decrease in integration exhibited a large dependence not only on the type of α-hydrogens but also on the nucleobase present in these compounds. In all cases, the adenine derivative (**2b**) showed the fastest rate and the thymine analogue (**2a**) the slowest one. If I_t is the integration obtained for a given signal at a time t, and I_{eq} is the integration at the *H-D* exchange equilibrium (at one week), then the linear graphics ln (I_t-I_{eq}) vs t (Figure 3) indicate that the kinetic is of

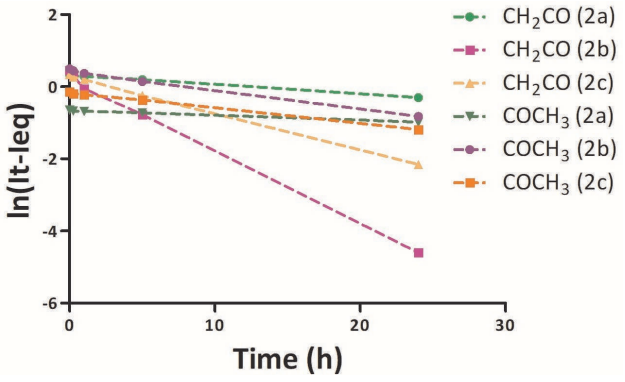

Figure 3. ln(I_t-I_{eq}) vs t curves of (CH_2CO) and ($COCH_3$) ^{1}H NMR signals of compounds **2a-c** in D_2O.

first order with respect to the ketones **2a-c** both for the exchange of deuterium in CH_2 and in CH_3.Then, the deuteration velocity follows the kinetic formula

$$v = k_{ap}C \quad (1)$$

where k_{ap} is the apparent rate constant and C is the total concentration of substrate. Since the concentration of the compounds and the integration of the signals are proportional

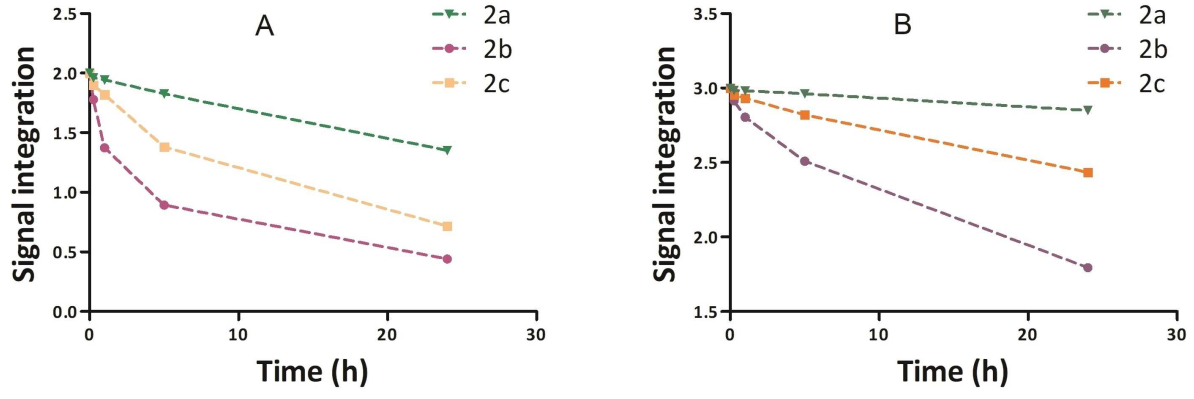

Figure 2. (A) (CH_2CO) and (B) ($COCH_3$) ^{1}H NMR signals integration over time of compounds **2a-c** in D_2O.

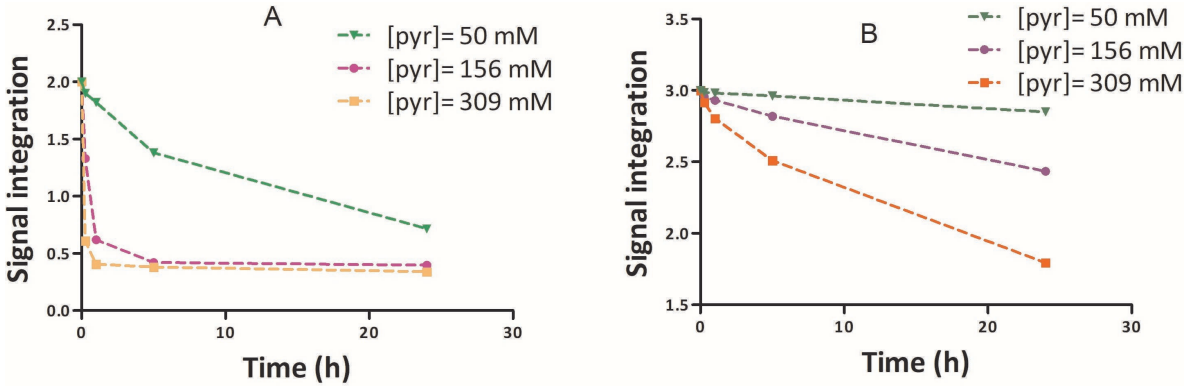

Figure 4. (A) (CH_2CO) and (B) ($COCH_3$) ^{1}H NMR signals integration over time of compound **2c** in D_2O at 3 different pyrrolidine concentration.

to each other, the curves C_t vs t and I_t vs t afford the same k_{ap} value. Then, C_t can be described as

Table 1. Parameters corresponding to the exponential adjustments of the integration vs time curves of the signals of the exchangeable protons of compounds **2a-c** at different pyrrolidine concentrations

Signal	Compound	Pyr (mM)	I_0	I_{eq}	a (h^{-1})	R^2
CH_2CO	**2a**	50	1.98 ± 0.02	0.59 ± 0.01	0.025 ± 0.001	0.9994
		200	2.0 ± 0.1	0.32 ± 0.07	0.5 ± 0.1	0.9785
		351	1.97 ± 0.06	0.31 ± 0.03	0.83 ± 0.08	0.9939
	2b	50	1.9 ± 0.1	0.45 ± 0.08	0.29 ± 0.08	0.9649
		182	2.0 ± 0.1	0.88 ± 0.07	2.4 ± 0.9	0.9167
		344	2.00 ± 0.01	0.43 ± 0.01	13.9 ± 0.2	0.9999
	2c	50	1.97 ± 0.03	0.61 ± 0.02	0.11 ± 0.01	0.9979
		156	2.00 ± 0.04	0.39 ± 0.02	2.1 ± 0.1	0.991
		309	2.00 ± 0.03	0.36 ± 0.01	7.6 ± 0.5	0.9997
$COCH_3$	**2a**	50	2.98 ± 0.02	2.37 ± 0.02	0.011 ± 0.001	0.9989
		200	3.02 ± 0.09	0.47 ± 0.06	0.062 ± 0.005	0.9965
		351	2.9 ± 0.1	0.3 ± 0.1	0.09 ± 0.01	0.9902
	2b	50	2.9 ± 0.1	1.34 ± 0.09	0.049 ± 0.008	0.9824
		182	3.0 ± 0.2	0.9 ± 0.1	2.3 ± 0.8	0.9758
		344	3.0 ± 0.1	0.63 ± 0.07	8.2 ± 0.3	0.9806
	2c	50	3.0 ± 0.3	2.1 ± 0.2	0.04 ± 0.01	0.992
		156	3.1 ± 0.2	0.6 ± 0.1	0.8 ± 0.1	0.9753
		309	3.01 ± 0.07	0.48 ± 0.03	2.7 ± 0.2	0.997

$$C_t = (C_o - C_{eq})\, e^{-kapt} + C_{eq} \quad (2)$$

where C_o, C_{eq} and C_t are the initial, at equilibrium and at time t concentrations, respectively. An analogous relationship is valid for integrations.

To evaluate the role of pyrrolidine in the keto-enol equilibrium, ^{1}H NMR spectra of compounds **2a-c** in D_2O at different pyrrolidine concentrations over time were analysed. Figure 4 shows the integration of ($COCH_3$) and (CH_2CO) signals as a function of time for **2c** at three concentrations of pyrrolidine: 50 mM, 156 mM, and 309 mM. As can be seen, the addition of base produced an increase in the *H-D* exchange rate for both groups. These data and those obtained from **2a** and **2b** were adjusted according to the equation:

$$I_t = (I_0\text{-}I_{eq})\, e^{-a\,t} + I_{eq} \quad (3)$$

Table 1 summarises the calculated parameters I_0, I_{eq} and a. The initial velocity (v_0) for each system was calculated from the slope [(I_0-I_{eq})a] of the corresponding exponential curves at initial times. The ratio v_0/I_0 afforded k_{ap} for each base, which depends on the concentration of pyrrolidine. The obtained results are shown in Table 2. The curves of k_{ap} vs pyrrolidine concentration [pyr] (Figure 5) clearly show that, in the case of **2b** and **2c**, the kinetics are of second order with respect to the base concentration; while for **2a** the kinetic is of first order. Then,

$$k_{ap} = k\,[pyr]^2 \text{ for } \mathbf{2b} \text{ and } \mathbf{2c} \quad (4)$$

$$k_{ap} = k\,[pyr] \text{ for } \mathbf{2a} \quad (5)$$

Finally, the calculated specific velocity constants k are shown in the last column of Table 2. The resulting rate laws are

$$v = k\,[S]\,[pyr]^2 \text{ for } \mathbf{2b} \text{ and } \mathbf{2c} \quad (6)$$

$$v = k\,[S]\,[py] \text{ for } \mathbf{2a} \quad (7)$$

were [S] is the substrate concentration. These results suggest that the nucleobase is playing a relevant role in the *H-D*

Table 2. Kinetic parameters for ($COCH_3$) and (-CH_2CO) signals evolution of compounds **2a-c** at different pyrrolidine concentrations

Signal	Nucleobase	Pyr (mM)	v_0 (s^{-1})	k_{ap} (s^{-1})	k ($M^{-1}h^{-1}$)
CH_2CO	Adenine	50	0.4 ± 0.1	0.22 ± 0.06	88 ± 9
		182	2.6 ± 0.9	1.3 ± 0.5	
		344	21.8 ± 0.3	10.9 ± 0.1	
	Cytosine	50	0.15 ± 0.01	0.077 ± 0.006	65 ± 1
		156	3.3 ± 0.1	1.7 ± 0.1	
		309	12.4 ± 0.8	6.2 ± 0.4	
	Thymine	50	0.035 ± 0.001	0.0177 ± 0.0006	2.0 ± 0.2
		200	0.9 ± 0.2	0.46 ± 0.09	
		351	1.4 ± 0.2	0.70 ± 0.08	
$COCH_3$	Adenine	50	0.08 ± 0.01	0.027 ± 0.004	54 ± 1
		182	4.7 ± 0.8	1.6 ± 0.6	
		344	19.8 ± 0.9	6.5 ± 0.6	
	Cytosine	50	0.04 ± 0.02	0.012 ± 0.006	24.0 ± 0.8
		156	2.1 ± 0.5	0.7 ± 0.1	
		309	6.8 ± 0.5	2.3 ± 0.2	
	Thymine	50	0.0066 ± 0.0007	0.0022 ± 0.0002	0.24 ± 0.02
		200	0.16 ± 0.01	0.052 ± 0.004	
		351	0.24 ± 0.03	0.08 ± 0.01	

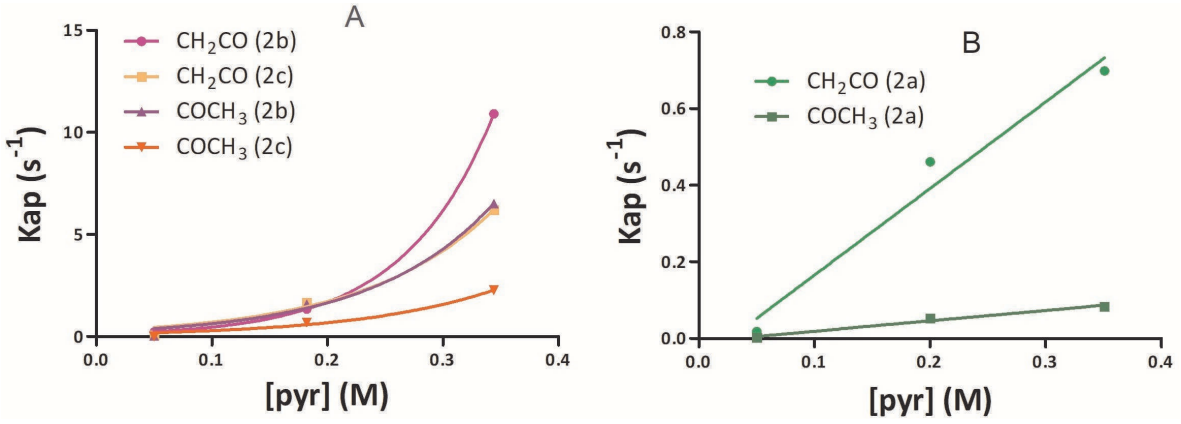

Figure 5. Curves of k_{ap} vs pyrrolidine concentration of (CH_2CO) and ($COCH_3$) ^1H NMR signals of compounds (A) **2b** and **2c** and (B) **2a** in D_2O.

exchange mechanism. In this sense, one important difference among the three nucleobases is their acidity, being thymine (pK_a 9.9) much less acidic than adenine (pK_a 3.5) and cytosine (pK_a 4.2). Assuming that the acidity of the bases is not affected by the presence of the chain bound to the nitrogen, it can be presumed that both adenine and cytosine derivatives **2b** and **2c** will be easily deprotonated by the pyrrolidine (pK_b 2.7) present in the medium while the derivative of thymine **2a** will be mostly in neutral form.

Proposed keto-enol equilibrium mechanisms

Based on the obtained spectroscopic and kinetic results, it can be concluded that the *H-D* exchange is consistent with the existence of keto-enol equilibrium in compounds **2a-c**. The mechanism by which it occurs must meet the following experimental data: i) should be of first order with respect to the substrate; ii) should be of order 2 with respect to pyrrolidine for cytosine and adenine derivatives, but of order 1 for the thymine analogue, and iii) the substrate should play a role that depends on its acid-base strength.

Then, the proposed mechanism for **2a** corresponds to a classical base-catalysed deuteration mechanism in protic media: subtraction of a proton adjacent to a carbonyl group by pyrrolidine and subsequent acid-base reaction between the generated carbanion and D_2O. In contrast, in the case of **2b** and **2c**, we propose a first fast acid-base equilibrium step followed by the addition of pyrrolidine to the carbonyl group with subsequent proton subtraction by a second pyrrolidine molecule (hence the second order). Scheme 3 shows the detailed proposal using **2c** as model. These three steps are followed by a fast tautomerisation step that leads to the deuterated keto forms.

A possible explanation about the role played by the nitrogenous base, leading to different mechanisms, could be focused on the stability of the addition intermediate produced in step 2 (Scheme 3). In order to support this assumption, theoretical calculations were carried out. The optimised structures of the three anions show a hydrogen bond between

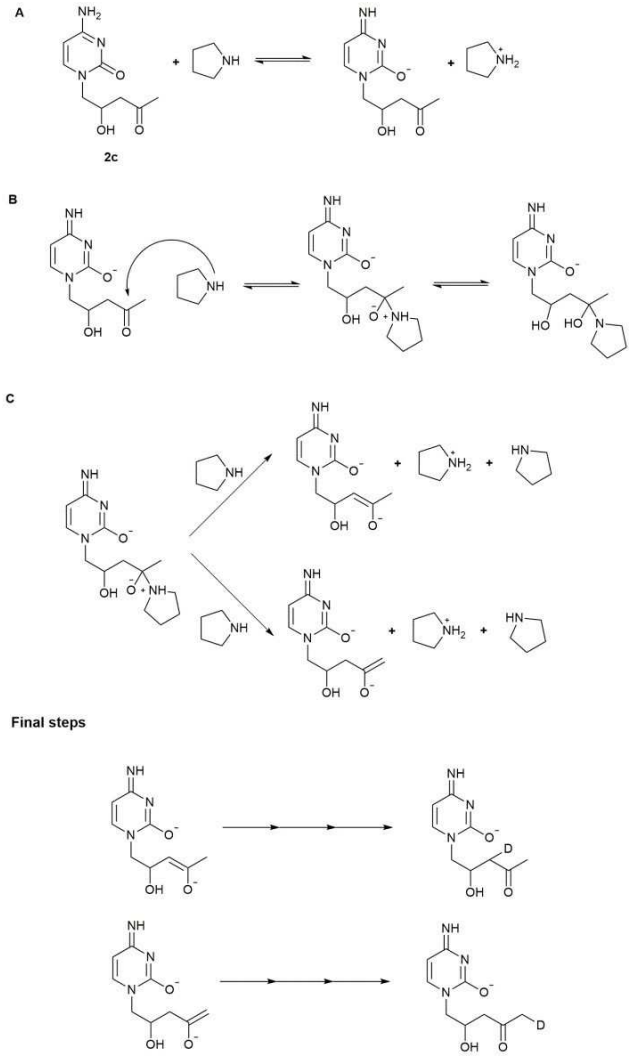

Scheme 3. Proposed mechanism for deuteration of compound **2c**. Step A: fast acid/base equilibrium between **2c** and pyrrolidine. Step B: fast addition of pyrrolidine to the intermediate anion. Step C: deprotonation by a second pyrrolidine molecule and enolate formation by pyrrolidine elimination (rate-determining step). The final steps lead to fast deuteration of the enolate and formation of the keto tautomer.

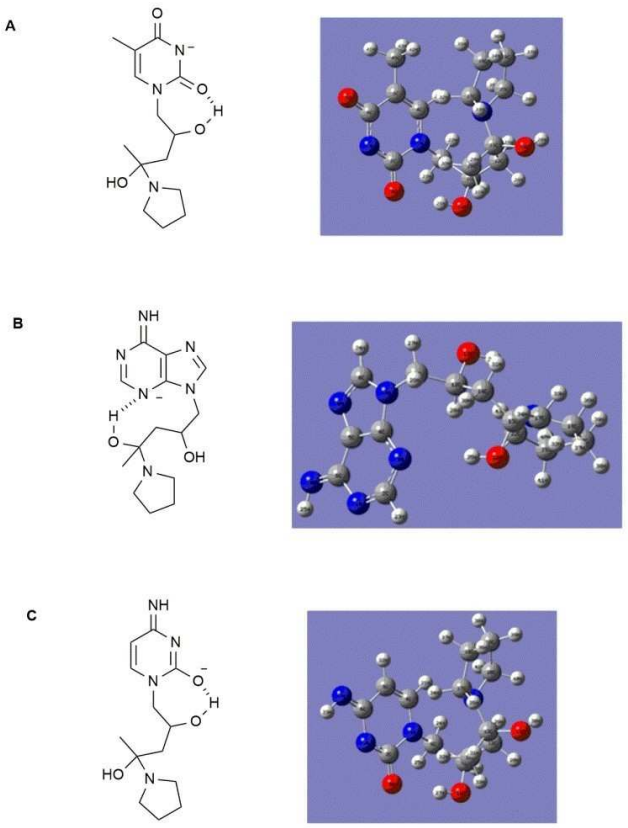

Figure 6. Optimised structures of the anionic intermediates formed in step B (Scheme 3), calculated at level of B3LYP/6-31G(d,p) with PCM model water. (A) **2a**; (B) **2b**; (C) **2c**. Internal hydrogen bonds are shown in dashed lines.

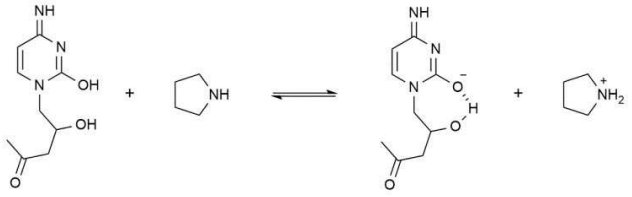

Scheme 4. Acid-base equilibrium used to estimate the stabilization energy in the anionic intermediate (depicted for compound **2c**).

one OH of the alkyl chain and one of the heteroatoms of the nucleobase (Figure 6). The energy involved in that hydrogen bond would improve the stability of the anion with respect to the neutral intermediate.

One possible way of evaluating the different stabilisation produced by hydrogen bonds in the three intermediates is calculating the energy involved in their deprotonation. Scheme 4 shows acid-base equilibrium between compound **2c** and pyrrolidine (the equilibria for **2a** and **2b** are analogous). The energy of the four structures involved in the chemical equilibrium shown in Scheme 4 were calculated by means of B3LYP/6-31G(d,p) using a PCM model in water solvent.

The energy difference obtained by this method afforded 0.1 kcal/mol, −4.2 kcal/mol and −2.0 kcal/mol for **2a**, **2b** and **2c**, respectively. Since the anion of the thymine derivative is the less stabilised and, hence, is formed in a small amount (due mainly to its high pK_a), the intermediate does not occur and, subsequently, *H-D* exchange follows the classic basic catalysis pathway, of order 1 with respect to both substrates and slower than in the case of adenine and cytosine derivatives.

Conclusions

Three potentially pharmacological active acyclic nucleoside analogues (**2a-c**) were synthesised in high yields from acetone and 2-oxoethyl derivatives of the corresponding nucleobases by an organocatalysed approach using pyrrolidine as organocatalyst. These compounds, consisting of a β-hydroxyketone chain attached to a heterocyclic nitrogen of the nucleobases,

showed *H-D* exchange of the α-hydrogens of the carbonyl group as consequence of keto-enol equilibrium in basic pyrrolidine medium. The theoretical and experimental results suggest that the mechanism through which the exchange occurs is different according to the pK_a of the nucleobase present in those compounds. When the base was thymine, a classical base-catalysed mechanism takes place. In contrast, when more acidic bases are involved, such as adenine and cytosine, a fast and multistep mechanism was proposed where the stability of the anion formed by addition of pyrrolidine plays a key role.

Supporting Information Summary

Experimental details, compound data and characterisation and copies of ^{1}H and ^{13}C NMR spectra are provided in Supporting Information

Acknowledgements

This study was supported by a grant of Universidad Nacional de Quilmes, Facultad de Ciencias Exactas (Universidad Nacional de La Plata) and ANPCyT (PICT 2012-0811). ESL and AMI are members of the Scientific Researcher Career of CONICET. MG is CONICET fellow.

Conflict of Interest

The authors declare no conflict of interest.

Keywords: Acyclic nucleosides · Aldol reaction · *H-D* exchange · Organocatalysis · Tautomerism

[1] P. Jordheim, D. Durantel, F. Zoulim, C. Dumontet, *Nat. Rev. Drug. Discov.* **2013**, *12*, 447–464.
[2] E. De Clercq, G. Li, *Clin. Microbiol. Rev.* **2016**, *29*, 695–747.
[3] K. L. Seley-Radtke, M. K. Yates, *Antiviral Res.* **2018**, *154*, 66–86.
[4] G. B. Elion, P. A. Furman, J. A. Fyfe, P. de Miranda, L. Beauchamp, H. J. Schaeffer, *Proc. Natl. Acad. Sci. USA* **1977**, *74*, 5716–5720.
[5] E. Głowacka, J. Balzarini, G. Andrei, R. Snoeck, D. Schols, D. G. Piotrowska, *Med. Chem.* **2014**, *22*, 3629–3641.
[6] S. Malthum, N. Polkam, T. R. Allaka, K. Chepuri, J. S. Anireddy, *Tetrahedron Lett.* **2017**, *58*, 4166–4168.
[7] M. Palazzolo, M. Pérez-Sánchez, A. M. Iribarren, E. Lewkowicz, P. Domínguez de María, *Tetrahedron Lett.* **2012**, *53*, 6797–6800.
[8] M. Palazzolo, M. Nigro, A. M. Iribarren, E. Lewkowicz, *Eur. J. Org. Chem.* **2016**, *5*, 921–924.
[9] a) M. Dondoni, A. Massi, *Angew. Chem. Int. Ed.* **2008**, *47*, 4638–4660; b) P. Renzi, M. Bella, *M. Chem. Commun.* **2012**, *48*, 6881–6896; c) P. Domínguez de María, P. Bracco, L. F. Castelhano, G. Bargeman, *ACS Catal.* **2011**, *1*, 70–75; d) S. Shanmuganathan, L. Greiner, P. Domínguez de María, *Tetrahedron Lett.* **2012**, *51*, 6670–6672; e) G. R. Qu, H. L. Zhang, H. Y. Niu, Z. K. Xué, X. X. Lv, H. M. Guo, *Green Chem.* **2012**, *14*, 1877–1879.
[10] M. Kumar, A. Kumar, M. Rizvi, B. A. Shah, *RSC Adv.* **2015**, *5*, 55926–55937.
[11] M. M. Heravi, V. Zadsirjan, M. Dehghani, N. Hosseintash, *Tetrahedron Asymmetry* **2017**, *28*, 587–707.
[12] P. Clapes, W. D. Fessner, G. A. Sprenger, A. K. Samland, *Curr. Opin. Chem. Biol.* **2010**, *14*, 154–167.
[13] V. Bisai, A. Bisai, S. Singh, *Tetrahedron* **2012**, *68*, 4541–4580.
[14] C. A. Busacca, D. R. Fandrick, J. J. Song, C. H. Senanayake, *Adv. Synth. Catal.* **2011**, *353*, 1825–1864.
[15] B. List, R. A. Lerner, C. F. Barbas III, *J. Am. Chem. Soc.* **2000**, *122*, 2395–2396.
[16] B. B. Ahuja, A. Sudalai, *Tetrahedron Asymmetry* **2015**, *26*, 548–552.
[17] H. Lu, J. Bai, J. Xu, T. Yang, X. Lin, J. Li, F. Ren, *Tetrahedron* **2015**, *71*, 2610–2615.
[18] C. Nájera, M. Yus, *Tetrahedron Lett.* **2015**, *56*, 2623–2633.
[19] D. G. Crivoi, R. A. Miranda, E. Finocchio, J. Llorca, G. Ramis, J. E. Sueiras, A. M. Segarra, F. Medina, *Appl. Catal. A Gen.* **2016**, *519*, 116–129.
[20] S. L. Laurella, D. D. Colasurdo, D. L. Ruiz, P. E. Allegretti, Ed. Bentham eBooks **2017**, *6*, 1–46.
[21] H. O. House, *J. Chem. Educ.* **1972**, *595*, 8–10.
[22] a) Y. Chiang, A. J. Kresge, M. Capponi, J. Wirz, *Helv. Chim.* **1986**, *69*, 1331–1332; b) B. Capon, C. Zucco, *J. Am. Ceram. Soc.* **1982**, *104*, 7567–7572.
[23] C. C. Su, C. K. Lin, C. C. Wu, M. H. Lien, *J. Phys. Chem. A* **1999**, *103*, 3289–3293.
[24] H. Jarret, M. Sadler, J. Shoolery, *J. Chem. Phys.* **1953**, *21*, 2092–2093.
[25] R. L. Lintvedt, Jr. H. F. Holtzclaw, *Inorg. Chem.* **1966**, *5*, 239–241.
[26] R. L. Lintvedt, Jr. H. F. Holtzclaw, *J. Am. Chem. Soc.* **1966**, *88*, 2713–2716.
[27] C. Haddon, *J. Am. Chem. Soc.* **1980**, *102*, 1807–1811.
[28] M. J. Nigro, J. I. Brardinelli, E. S. Lewkowicz, A. M. Iribarren, S. L. Laurella, *J. Mol. Struct.* **2017**, *1144*, 49–57.
[29] R. A. Sayle, J. Comput, *Aided Mol Des* **2010**, *24*, 485–496.

Submitted: August 13, 2018
Accepted: November 23, 2018